Electronic Supplementary Material (ESI) for CrystEngComm.

Electronic supporting information

LiquidReactionCell – a versatile setup for *in situ* synchrotron studies of compounds in liquid suspension and solution

Henrik S. Jeppesen[1], Ida G. Nielsen[2], Jens Christian Kondrup[3], Justus Just[4] and Nina Lock[5*]

[1]Sino-Danish Center for Research and education (SDC), Interdisciplinary Nanoscience Center (iNANO), Aarhus University, Gustav Wieds Vej 14, DK-8000 Aarhus C, Denmark.

[2]Deutsches Elektronen-Synchrotron (DESY), Notkestraße 85, D-22607 Hamburg, Germany

[3]Department of Chemistry, Aarhus University, Langelandsgade 140, DK-8000 Aarhus C, Denmark.

[4]MAX IV Laboratory, Fotongatan 2, 224 84 Lund, Sweden

[5]Carbon Dioxide Activation Center (CADIAC), Department of Biological and Chemical Engineering and iNANO, Åbogade 40, DK-8200 Aarhus N, Denmark

*corresponding author: nlock@bce.au.dk

1. Mounting methods for the LRC

1.1 Mounting for XAS on Balder at the MAX IV Laboratory

The LRC was mounted at Balder by using a 3D printed holder and a rubber band and two screws (see manuscript Fig. 2c-d). The mount allows for vigorous stirring of the suspension while keeping the LRC at a fixed position. The cell was rotated 45° to the beam direction allowing for transmission through of the cell and collection of the fluorescence signal at 90° to the incident beam. The technical drawings of the sample holder are displayed in Fig. S1.

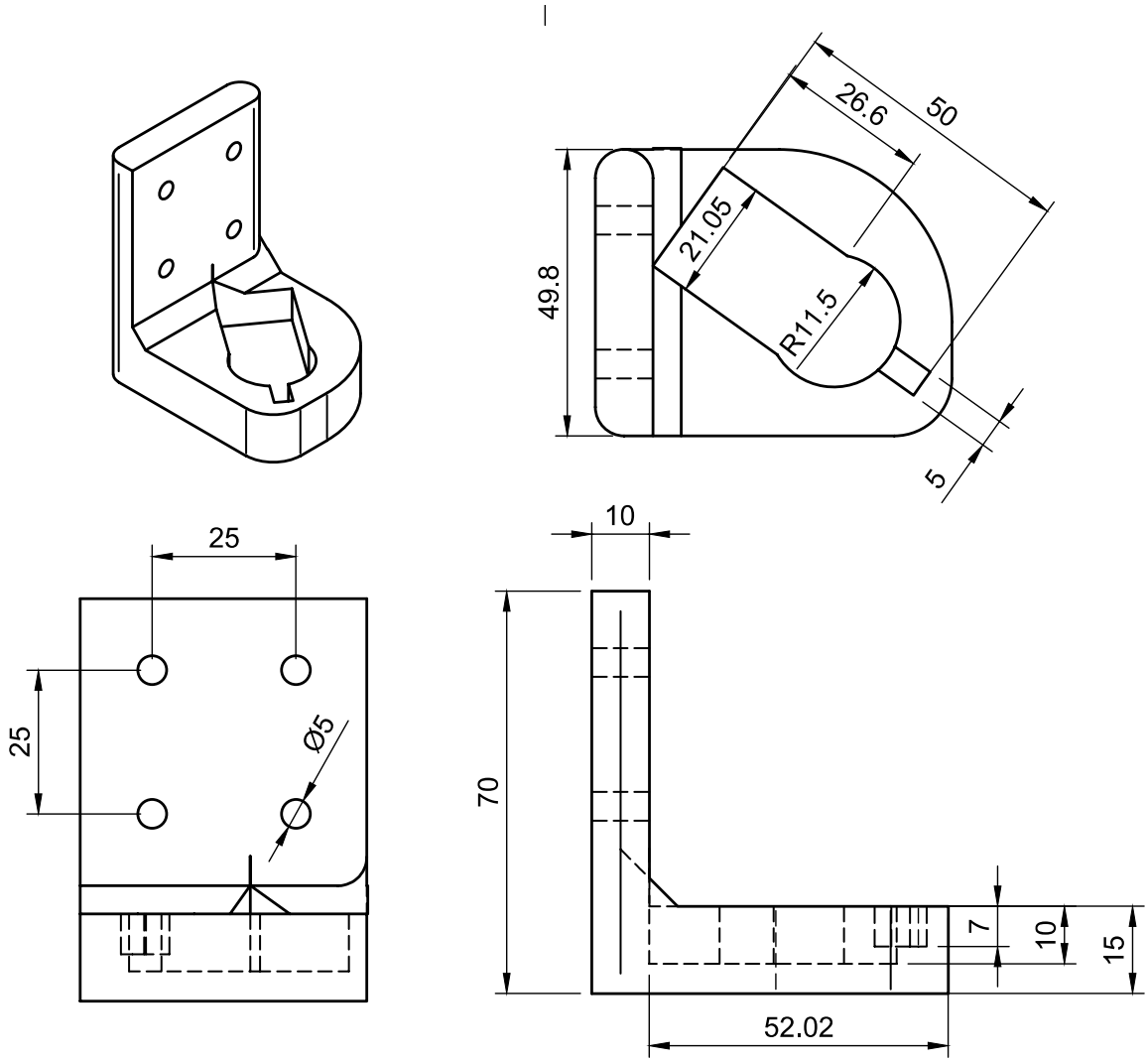

Fig. S1. Technical drawings of the LRC holder designed for Balder, MAX IV Laboratory.

1.2 Mounting for total scattering experiments on P02.1 at PETRA III

For total scattering experiments at P02.1 at PETRA III, DESY the protection rod of the LRC setup was clamped to a chemical stand. To ensure a consistent positioning of the LRC in the centre of the magnetic stirrer, an alignment tool was designed. In Fig. S2 and Fig. S3 technical drawings of the LRC alignment tool and the capillary alignment tool is shown. The latter is used for mounting of capillaries, e.g. for alignment purposes. The two tools allow data collection of the LRC and capillary in the exact same position, ensuring a fixed sample-to-detector distance. No capillary spinning is possible with this setup.

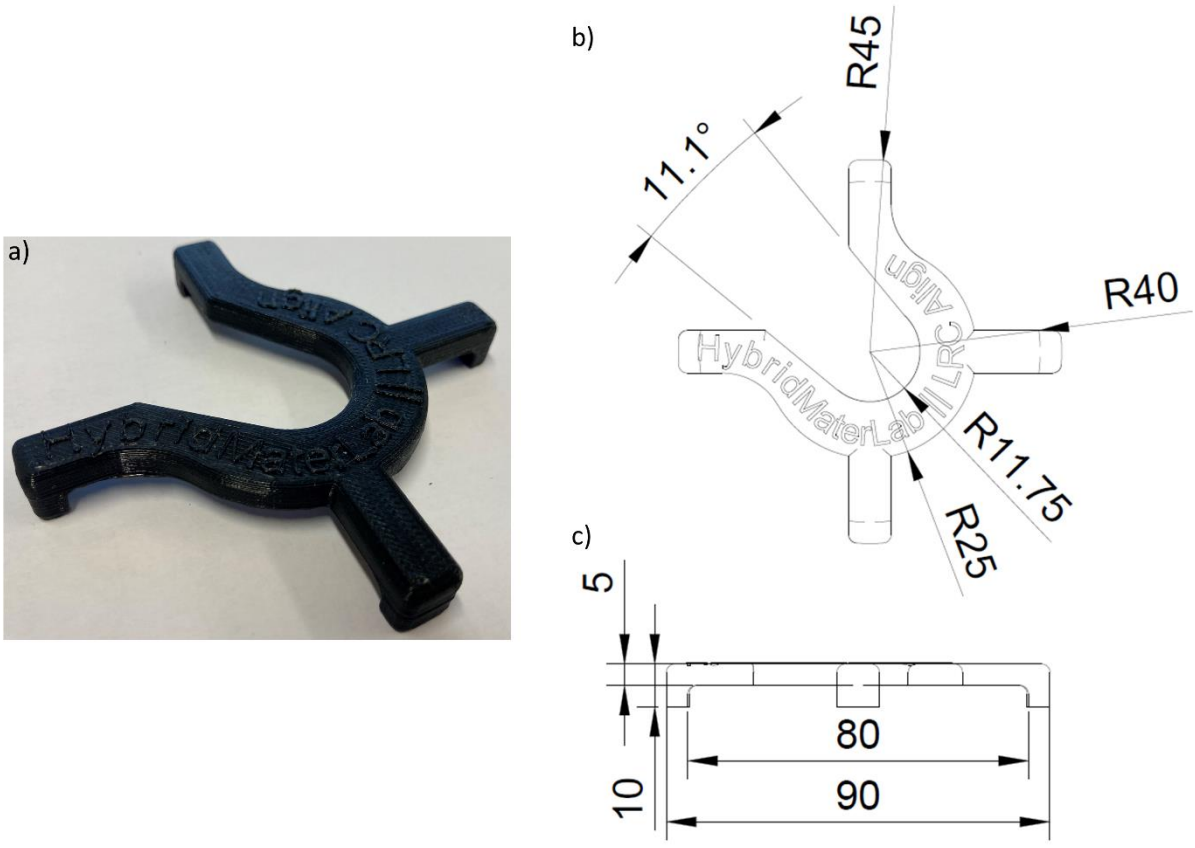

Fig. S2. a) Photo of the LRC alignment tool and technical drawings of the same holder viewed from b) the top, and c) the side.

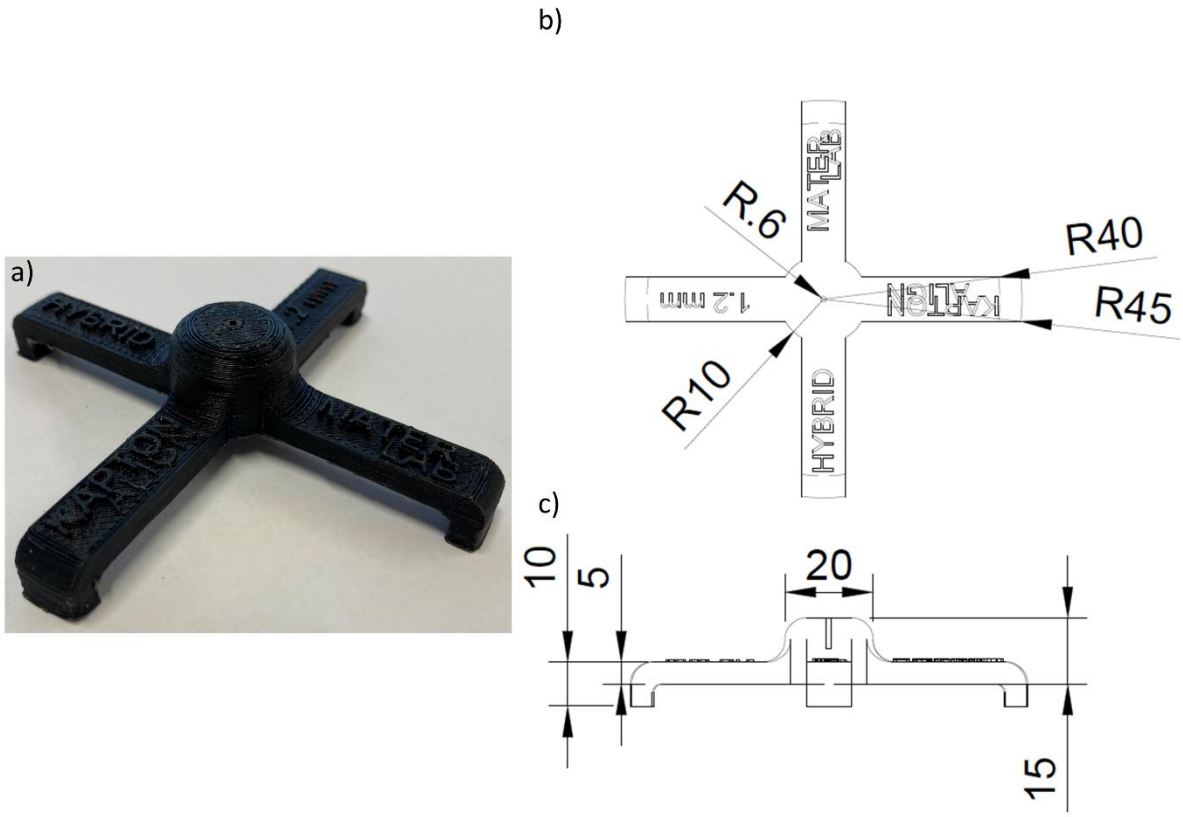

Fig. S3. a) Photo of the capillary alignment tool, with technical drawings of the holder viewed from b) the top, and c) the side

2. Liquid addition/exchange

In Fig. S4 liquid addition/exchange is demonstrated with an aqueous solution of methylene blue. Using a New-Era syringe pump (NE-1000) a total of 0.9 mL methylene blue solution was injected into the LRC. The injected volume was determined by weight and matched the volume "pushed out" of the cell *via* the outlet needle.

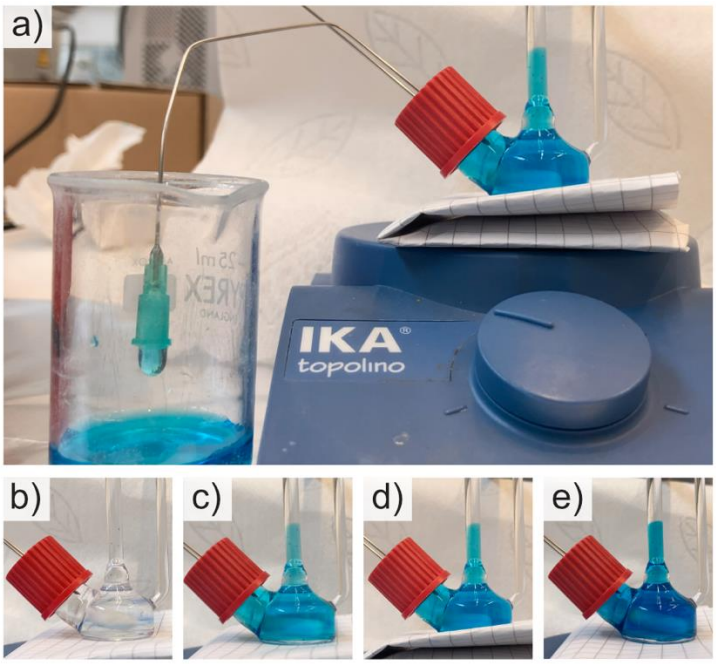

Fig. S4. Liquid addition/exchange experiments of the LRC using a methylene blue solution. a) General setup with injection and outlet needle mounted through the septum. The injection needle is connected to a syringe pump. b)-e) Injection of methylene blue solution (0.9 mL in total) under stirring in steps of 0.3 mL.

3. MATLAB scripts for transmission calculations

The scripts used to estimate transmission through the cell and solvent as presented in the manuscript Fig. 3 is shown below. The scripts have been developed in MATLAB_R2020b.

3.1 Input for X-ray absorption calculations

Table S1: Densities and radii used in the absorption calculations.

	Composition	Density (g/cm^3)	Radius (mm)
Borosilicate 3.3	SiO_2 mixed*	2.2	
Water	H_2O	1	1.75
iPrOH	C_3H_8O	0.785	1.75

*12% B_2O_3, 80% SiO_2, 4% Na_2O, 2% Al_2O_3 (by mass)

3.2 Transmission calculations in the X-ray illumination zone

The script for calculating the transmission in the X-ray illumination zone was set up to include the glass and the solvent inside the capillary. Attenuation factors were calculated using XCOM made by NIST[1]. In the final part of the script, an empty template has been included for easy calculation of the transmission due to other solvents. The X-ray attenuation was calculated using the following equation

$$I = I_0 \cdot e^{-\mu_m \rho d}$$

where I_0 and I is the intensity of the incoming and transmitted beam, respectively μ_m is the attenuation factor in $cm^2 \cdot g^{-1}$, ρ is the density of the medium, and d is the distance travelled.

```
function attenuation
clear all; close all; clc
[S_length,H2O,IPA,B_SIL]=numbers;

%Calculated with: https://physics.nist.gov/PhysRefData/Xcom/html/xcom1.html
%list of energies can be found in the bottom of the document to make this match with the rest
%When exporting interaction values, please select all outputs and choose "tab" as the delimiter

I_WATER_SETUP=ABS_SETUP(H2O,S_length,B_SIL);
plot(H2O.dat(:,1),I_WATER_SETUP,'b.-','MarkerSize',13)
hold on
I_IPA_SETUP=ABS_SETUP(IPA,S_length,B_SIL);
plot(IPA.dat(:,1),I_IPA_SETUP,'r.-','MarkerSize',13)

I_GLASS=ABS_GLASS(S_length,B_SIL);
plot(B_SIL.dat(:,1),I_GLASS,'k.-','MarkerSize',13)


legend('Cell + water','Cell + IPA','Cell Only','location','southeast')
xlabel('X-ray Energy (keV)')
ylabel('Transmission (%)')
ylim([0 100])
end
```

```
function I=ABS(I0,d,mu)
I=I0.*exp(-mu*d);
end

function I3=ABS_SETUP(medium,S_length,B_SIL)
I0=100;
I1=ABS(I0,S_length.glass,B_SIL.mu); %absorption by entering glass cell
I2=ABS(I1,S_length.medium,medium.mu); %absorption by the medium in the centre of the cell
I3=ABS(I2,S_length.glass,B_SIL.mu); %absorption when leaving the cell


end

function I2=ABS_GLASS(S_length,B_SIL)
I0=100;
I1=ABS(I0,S_length.glass,B_SIL.mu); %absorption by entering glass cell
I2=ABS(I1,S_length.glass,B_SIL.mu); %absorption when leaving the cell
end


function [S_Length,H2O,IPA,B_SIL]=numbers
%% SETUP LENGTHS
S_Length=[];
S_Length.glass=0.001; %cm
S_Length.medium=0.35; %cm


%% WATER
H2O=[];
H2O.title='water';
H2O.rho=1.0; %g/cm
%       |     SCATTERING      |          |   Pair Production    |  Total Attenuation
%Photon   | Coherent  | Incoher.  | Photoel.  | Nuclear   | Electron  | Tot. w/   | Tot. wo/
%Energy   | Scatter.  | Scatter.  | Absorb.   | Pr. Prd.  | Pr. Prd.  | Coherent  | Coherent
%MeV     | cm2/g     | cm2/g     | cm2/g     | cm2/g     | cm2/g     | cm2/g     | cm2/g
H2O.dat=...
[1.000E-03  1.372E+00   1.319E-02   4.076E+03   0.000E+00   0.000E+00   4.077E+03   4.076E+03
2.000E-03   1.150E+00   4.184E-02   6.162E+02   0.000E+00   0.000E+00   6.173E+02   6.162E+02
3.000E-03   9.087E-01   7.075E-02   1.919E+02   0.000E+00   0.000E+00   1.928E+02   1.919E+02
4.000E-03   7.082E-01   9.430E-02   8.197E+01   0.000E+00   0.000E+00   8.277E+01   8.207E+01
5.000E-03   5.579E-01   1.123E-01   4.192E+01   0.000E+00   0.000E+00   4.259E+01   4.203E+01
6.000E-03   4.489E-01   1.259E-01   2.407E+01   0.000E+00   0.000E+00   2.464E+01   2.419E+01
7.000E-03   3.693E-01   1.361E-01   1.499E+01   0.000E+00   0.000E+00   1.550E+01   1.513E+01
8.000E-03   3.102E-01   1.440E-01   9.919E+00   0.000E+00   0.000E+00   1.037E+01   1.006E+01
9.000E-03   2.653E-01   1.501E-01   6.875E+00   0.000E+00   0.000E+00   7.291E+00   7.025E+00
1.000E-02   2.305E-01   1.550E-01   4.944E+00   0.000E+00   0.000E+00   5.330E+00   5.099E+00
1.100E-02   2.029E-01   1.591E-01   3.664E+00   0.000E+00   0.000E+00   4.026E+00   3.823E+00
1.200E-02   1.806E-01   1.624E-01   2.783E+00   0.000E+00   0.000E+00   3.126E+00   2.946E+00
1.300E-02   1.621E-01   1.653E-01   2.160E+00   0.000E+00   0.000E+00   2.487E+00   2.325E+00
1.400E-02   1.465E-01   1.678E-01   1.706E+00   0.000E+00   0.000E+00   2.021E+00   1.874E+00
1.500E-02   1.333E-01   1.699E-01   1.369E+00   0.000E+00   0.000E+00   1.672E+00   1.539E+00
1.600E-02   1.219E-01   1.718E-01   1.114E+00   0.000E+00   0.000E+00   1.408E+00   1.286E+00
1.700E-02   1.119E-01   1.735E-01   9.174E-01   0.000E+00   0.000E+00   1.203E+00   1.091E+00
1.800E-02   1.032E-01   1.749E-01   7.636E-01   0.000E+00   0.000E+00   1.042E+00   9.385E-01
1.900E-02   9.547E-02   1.762E-01   6.417E-01   0.000E+00   0.000E+00   9.134E-01   8.179E-01
2.000E-02   8.856E-02   1.774E-01   5.439E-01   0.000E+00   0.000E+00   8.098E-01   7.213E-01
2.100E-02   8.237E-02   1.783E-01   4.646E-01   0.000E+00   0.000E+00   7.253E-01   6.430E-01
2.200E-02   7.679E-02   1.792E-01   3.997E-01   0.000E+00   0.000E+00   6.557E-01   5.789E-01
2.300E-02   7.174E-02   1.800E-01   3.461E-01   0.000E+00   0.000E+00   5.978E-01   5.261E-01
2.400E-02   6.717E-02   1.806E-01   3.015E-01   0.000E+00   0.000E+00   5.493E-01   4.821E-01
2.500E-02   6.301E-02   1.812E-01   2.640E-01   0.000E+00   0.000E+00   5.082E-01   4.452E-01
2.600E-02   5.921E-02   1.817E-01   2.324E-01   0.000E+00   0.000E+00   4.733E-01   4.141E-01
2.700E-02   5.574E-02   1.821E-01   2.055E-01   0.000E+00   0.000E+00   4.433E-01   3.876E-01
2.800E-02   5.256E-02   1.824E-01   1.826E-01   0.000E+00   0.000E+00   4.175E-01   3.650E-01
2.900E-02   4.963E-02   1.827E-01   1.628E-01   0.000E+00   0.000E+00   3.951E-01   3.455E-01
3.000E-02   4.694E-02   1.829E-01   1.458E-01   0.000E+00   0.000E+00   3.756E-01   3.286E-01
3.100E-02   4.445E-02   1.830E-01   1.309E-01   0.000E+00   0.000E+00   3.584E-01   3.140E-01
3.200E-02   4.215E-02   1.831E-01   1.180E-01   0.000E+00   0.000E+00   3.433E-01   3.012E-01
3.300E-02   4.002E-02   1.832E-01   1.067E-01   0.000E+00   0.000E+00   3.300E-01   2.899E-01
3.400E-02   3.804E-02   1.832E-01   9.679E-02   0.000E+00   0.000E+00   3.181E-01   2.800E-01
3.500E-02   3.621E-02   1.832E-01   8.802E-02   0.000E+00   0.000E+00   3.075E-01   2.713E-01
3.600E-02   3.450E-02   1.832E-01   8.026E-02   0.000E+00   0.000E+00   2.980E-01   2.635E-01
3.700E-02   3.291E-02   1.831E-01   7.336E-02   0.000E+00   0.000E+00   2.894E-01   2.565E-01
```

```
3.800E-02   3.143E-02   1.830E-01   6.722E-02   0.000E+00   0.000E+00   2.817E-01   2.502E-01
3.900E-02   3.004E-02   1.829E-01   6.172E-02   0.000E+00   0.000E+00   2.747E-01   2.446E-01
4.000E-02   2.874E-02   1.827E-01   5.680E-02   0.000E+00   0.000E+00   2.683E-01   2.395E-01
];

H2O.dat(:,1)=H2O.dat(:,1)*1000; %converting MeV to keV
H2O.mu=H2O.dat(:,7)*H2O.rho;

%% ISOPROPANOL
IPA=[];
IPA.title='isopropanol';
IPA.rho=0.786; %g/cc


%       |     SCATTERING       |          |   Pair Production     |  Total Attenuation
%Photon   | Coherent  | Incoher.  | Photoel.  | Nuclear   | Electron  | Tot. w/   | Tot. wo/
%Energy   | Scatter.  | Scatter.  | Absorb.   | Pr. Prd.  | Pr. Prd.  | Coherent  | Coherent
%MeV      | cm2/g     | cm2/g     | cm2/g     | cm2/g     | cm2/g     | cm2/g     | cm2/g
IPA.dat=...
[1.000E-03  1.093E+00   1.659E-02   2.547E+03   0.000E+00   0.000E+00   2.548E+03   2.547E+03
2.000E-03   8.682E-01   5.060E-02   3.657E+02   0.000E+00   0.000E+00   3.666E+02   3.657E+02
3.000E-03   6.564E-01   8.261E-02   1.113E+02   0.000E+00   0.000E+00   1.120E+02   1.114E+02
4.000E-03   4.996E-01   1.070E-01   4.691E+01   0.000E+00   0.000E+00   4.751E+01   4.701E+01
5.000E-03   3.908E-01   1.245E-01   2.376E+01   0.000E+00   0.000E+00   2.427E+01   2.388E+01
6.000E-03   3.155E-01   1.370E-01   1.354E+01   0.000E+00   0.000E+00   1.399E+01   1.368E+01
7.000E-03   2.619E-01   1.463E-01   8.382E+00   0.000E+00   0.000E+00   8.790E+00   8.528E+00
8.000E-03   2.224E-01   1.533E-01   5.517E+00   0.000E+00   0.000E+00   5.893E+00   5.670E+00
9.000E-03   1.923E-01   1.590E-01   3.807E+00   0.000E+00   0.000E+00   4.158E+00   3.966E+00
1.000E-02   1.687E-01   1.636E-01   2.727E+00   0.000E+00   0.000E+00   3.059E+00   2.891E+00
1.100E-02   1.497E-01   1.675E-01   2.014E+00   0.000E+00   0.000E+00   2.331E+00   2.182E+00
1.200E-02   1.340E-01   1.707E-01   1.526E+00   0.000E+00   0.000E+00   1.831E+00   1.697E+00
1.300E-02   1.208E-01   1.736E-01   1.181E+00   0.000E+00   0.000E+00   1.475E+00   1.354E+00
1.400E-02   1.095E-01   1.760E-01   9.308E-01   0.000E+00   0.000E+00   1.216E+00   1.107E+00
1.500E-02   9.980E-02   1.781E-01   7.454E-01   0.000E+00   0.000E+00   1.023E+00   9.236E-01
1.600E-02   9.130E-02   1.800E-01   6.053E-01   0.000E+00   0.000E+00   8.766E-01   7.853E-01
1.700E-02   8.382E-02   1.816E-01   4.975E-01   0.000E+00   0.000E+00   7.630E-01   6.791E-01
1.800E-02   7.720E-02   1.830E-01   4.134E-01   0.000E+00   0.000E+00   6.736E-01   5.964E-01
1.900E-02   7.132E-02   1.843E-01   3.469E-01   0.000E+00   0.000E+00   6.024E-01   5.311E-01
2.000E-02   6.606E-02   1.853E-01   2.936E-01   0.000E+00   0.000E+00   5.449E-01   4.789E-01
2.100E-02   6.135E-02   1.862E-01   2.505E-01   0.000E+00   0.000E+00   4.980E-01   4.367E-01
2.200E-02   5.710E-02   1.870E-01   2.152E-01   0.000E+00   0.000E+00   4.593E-01   4.022E-01
2.300E-02   5.326E-02   1.876E-01   1.861E-01   0.000E+00   0.000E+00   4.270E-01   3.737E-01
2.400E-02   4.979E-02   1.881E-01   1.620E-01   0.000E+00   0.000E+00   3.999E-01   3.501E-01
2.500E-02   4.664E-02   1.886E-01   1.417E-01   0.000E+00   0.000E+00   3.769E-01   3.303E-01
2.600E-02   4.377E-02   1.889E-01   1.246E-01   0.000E+00   0.000E+00   3.573E-01   3.136E-01
2.700E-02   4.116E-02   1.892E-01   1.101E-01   0.000E+00   0.000E+00   3.405E-01   2.993E-01
2.800E-02   3.876E-02   1.894E-01   9.773E-02   0.000E+00   0.000E+00   3.259E-01   2.871E-01
2.900E-02   3.657E-02   1.896E-01   8.709E-02   0.000E+00   0.000E+00   3.132E-01   2.767E-01
3.000E-02   3.455E-02   1.896E-01   7.791E-02   0.000E+00   0.000E+00   3.021E-01   2.676E-01
3.100E-02   3.269E-02   1.897E-01   6.995E-02   0.000E+00   0.000E+00   2.923E-01   2.596E-01
3.200E-02   3.098E-02   1.897E-01   6.301E-02   0.000E+00   0.000E+00   2.837E-01   2.527E-01
3.300E-02   2.940E-02   1.896E-01   5.693E-02   0.000E+00   0.000E+00   2.760E-01   2.466E-01
3.400E-02   2.793E-02   1.896E-01   5.160E-02   0.000E+00   0.000E+00   2.691E-01   2.412E-01
3.500E-02   2.657E-02   1.894E-01   4.690E-02   0.000E+00   0.000E+00   2.629E-01   2.363E-01
3.600E-02   2.531E-02   1.893E-01   4.274E-02   0.000E+00   0.000E+00   2.573E-01   2.320E-01
3.700E-02   2.413E-02   1.891E-01   3.904E-02   0.000E+00   0.000E+00   2.523E-01   2.282E-01
3.800E-02   2.303E-02   1.889E-01   3.575E-02   0.000E+00   0.000E+00   2.477E-01   2.247E-01
3.900E-02   2.201E-02   1.887E-01   3.281E-02   0.000E+00   0.000E+00   2.435E-01   2.215E-01
4.000E-02   2.105E-02   1.885E-01   3.018E-02   0.000E+00   0.000E+00   2.397E-01   2.187E-01   ];

IPA.dat(:,1)=IPA.dat(:,1)*1000; %converting MeV to keV
IPA.mu=IPA.dat(:,7)*IPA.rho;


%% Borosilicate
%composition by mass: 80.6% SiO2, 12.6% B2O3, 4.2% Na2O, 2.2% Al2O3
B_SIL=[];
B_SIL.title='Borosilicate glass';
B_SIL.rho=2.2; %g/cc
```

```
%        |     SCATTERING      |          |   Pair Production    |  Total Attenuation
%Photon   | Coherent  | Incoher.  | Photoel.  | Nuclear   | Electron  | Tot. w/   | Tot. wo/
%Energy   | Scatter.  | Scatter.  | Absorb.   | Pr. Prd.  | Pr. Prd.  | Coherent  | Coherent
%MeV      | cm2/g     | cm2/g     | cm2/g     | cm2/g     | cm2/g     | cm2/g     | cm2/g
B_SIL.dat=...
[1.000E-03  1.884E+00   1.077E-02   3.151E+03   0.000E+00   0.000E+00   3.153E+03   3.151E+03
2.000E-03   1.552E+00   3.118E-02   1.504E+03   0.000E+00   0.000E+00   1.506E+03   1.504E+03
3.000E-03   1.250E+00   5.078E-02   5.128E+02   0.000E+00   0.000E+00   5.141E+02   5.129E+02
4.000E-03   1.018E+00   6.727E-02   2.325E+02   0.000E+00   0.000E+00   2.336E+02   2.326E+02
5.000E-03   8.445E-01   8.079E-02   1.240E+02   0.000E+00   0.000E+00   1.249E+02   1.241E+02
6.000E-03   7.117E-01   9.184E-02   7.350E+01   0.000E+00   0.000E+00   7.430E+01   7.359E+01
7.000E-03   6.071E-01   1.009E-01   4.697E+01   0.000E+00   0.000E+00   4.768E+01   4.707E+01
8.000E-03   5.232E-01   1.085E-01   3.174E+01   0.000E+00   0.000E+00   3.237E+01   3.185E+01
9.000E-03   4.548E-01   1.149E-01   2.239E+01   0.000E+00   0.000E+00   2.296E+01   2.250E+01
1.000E-02   3.988E-01   1.203E-01   1.635E+01   0.000E+00   0.000E+00   1.687E+01   1.647E+01
1.100E-02   3.524E-01   1.250E-01   1.228E+01   0.000E+00   0.000E+00   1.276E+01   1.241E+01
1.200E-02   3.138E-01   1.290E-01   9.447E+00   0.000E+00   0.000E+00   9.890E+00   9.576E+00
1.300E-02   2.812E-01   1.326E-01   7.412E+00   0.000E+00   0.000E+00   7.826E+00   7.544E+00
1.400E-02   2.536E-01   1.357E-01   5.915E+00   0.000E+00   0.000E+00   6.304E+00   6.051E+00
1.500E-02   2.301E-01   1.384E-01   4.790E+00   0.000E+00   0.000E+00   5.159E+00   4.929E+00
1.600E-02   2.098E-01   1.408E-01   3.930E+00   0.000E+00   0.000E+00   4.281E+00   4.071E+00
1.700E-02   1.922E-01   1.430E-01   3.261E+00   0.000E+00   0.000E+00   3.596E+00   3.404E+00
1.800E-02   1.768E-01   1.449E-01   2.734E+00   0.000E+00   0.000E+00   3.055E+00   2.878E+00
1.900E-02   1.632E-01   1.465E-01   2.312E+00   0.000E+00   0.000E+00   2.622E+00   2.459E+00
2.000E-02   1.512E-01   1.480E-01   1.972E+00   0.000E+00   0.000E+00   2.272E+00   2.120E+00
2.100E-02   1.405E-01   1.494E-01   1.695E+00   0.000E+00   0.000E+00   1.985E+00   1.844E+00
2.200E-02   1.310E-01   1.506E-01   1.466E+00   0.000E+00   0.000E+00   1.748E+00   1.617E+00
2.300E-02   1.224E-01   1.516E-01   1.276E+00   0.000E+00   0.000E+00   1.550E+00   1.428E+00
2.400E-02   1.147E-01   1.525E-01   1.117E+00   0.000E+00   0.000E+00   1.384E+00   1.270E+00
2.500E-02   1.076E-01   1.534E-01   9.832E-01   0.000E+00   0.000E+00   1.244E+00   1.137E+00
2.600E-02   1.012E-01   1.541E-01   8.693E-01   0.000E+00   0.000E+00   1.125E+00   1.023E+00
2.700E-02   9.542E-02   1.548E-01   7.721E-01   0.000E+00   0.000E+00   1.022E+00   9.269E-01
2.800E-02   9.009E-02   1.553E-01   6.886E-01   0.000E+00   0.000E+00   9.341E-01   8.440E-01
2.900E-02   8.520E-02   1.558E-01   6.166E-01   0.000E+00   0.000E+00   8.576E-01   7.724E-01
3.000E-02   8.070E-02   1.563E-01   5.540E-01   0.000E+00   0.000E+00   7.910E-01   7.103E-01
3.100E-02   7.655E-02   1.567E-01   4.995E-01   0.000E+00   0.000E+00   7.327E-01   6.561E-01
3.200E-02   7.271E-02   1.570E-01   4.517E-01   0.000E+00   0.000E+00   6.814E-01   6.087E-01
3.300E-02   6.915E-02   1.573E-01   4.098E-01   0.000E+00   0.000E+00   6.362E-01   5.671E-01
3.400E-02   6.585E-02   1.575E-01   3.728E-01   0.000E+00   0.000E+00   5.962E-01   5.303E-01
3.500E-02   6.278E-02   1.577E-01   3.400E-01   0.000E+00   0.000E+00   5.605E-01   4.977E-01
3.600E-02   5.992E-02   1.579E-01   3.109E-01   0.000E+00   0.000E+00   5.287E-01   4.688E-01
3.700E-02   5.725E-02   1.580E-01   2.850E-01   0.000E+00   0.000E+00   5.002E-01   4.430E-01
3.800E-02   5.475E-02   1.581E-01   2.618E-01   0.000E+00   0.000E+00   4.746E-01   4.199E-01
3.900E-02   5.241E-02   1.582E-01   2.410E-01   0.000E+00   0.000E+00   4.516E-01   3.992E-01
4.000E-02   5.022E-02   1.582E-01   2.223E-01   0.000E+00   0.000E+00   4.307E-01   3.805E-01
];

B_SIL.dat(:,1)=B_SIL.dat(:,1)*1000; %converting MeV to keV
B_SIL.mu=B_SIL.dat(:,7)*B_SIL.rho;


%% Template for use of new solvent.
TEMP=[];
TEMP.title='Template';
TEMP.rho=1.0; %g/cc density

%        |     SCATTERING      |          |   Pair Production    |  Total Attenuation
%Photon   | Coherent  | Incoher.  | Photoel.  | Nuclear   | Electron  | Tot. w/   | Tot. wo/
%Energy   | Scatter.  | Scatter.  | Absorb.   | Pr. Prd.  | Pr. Prd.  | Coherent  | Coherent
%MeV      | cm2/g     | cm2/g     | cm2/g     | cm2/g     | cm2/g     | cm2/g     | cm2/g
TEMP.dat=...
[1.000E-03  1.884E+00   1.077E-02   3.151E+03   0.000E+00   0.000E+00   3.153E+03   3.151E+03
];

TMEP.dat(:,1)=TEMP.dat(:,1)*1000; %converting MeV to keV
TMEP.mu=TEMP.dat(:,7)*TEMP.rho;

    .
```

4. X-ray absorption spectroscopy

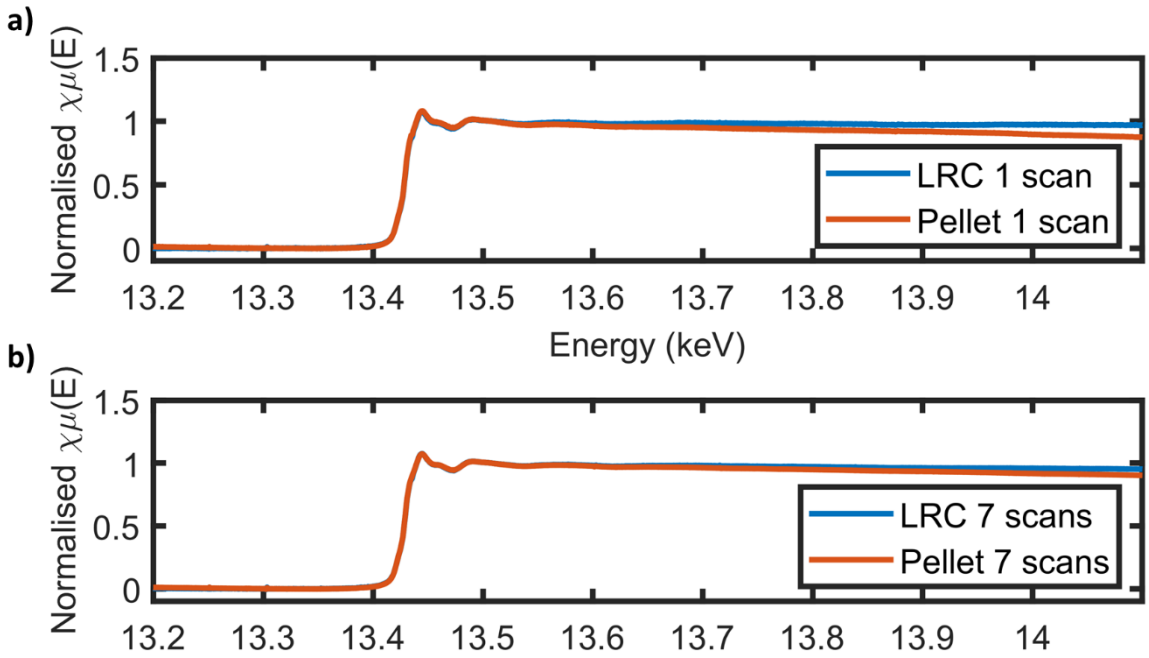

Fig. S5. Normalised absorption spectra collected on the Bi L^{III} edge on a pellet of $Bi_{24}O_{31}Cl_{10}$ (red) and a suspension of $Bi_{24}O_{31}Cl_{10}$ in the LRC (blue). a) A single spectrum of each, and b) 7 averaged spectra of each. A small difference is observed between the data collected in the LRC and on the pellet. This difference is reduced for the averaged spectra.

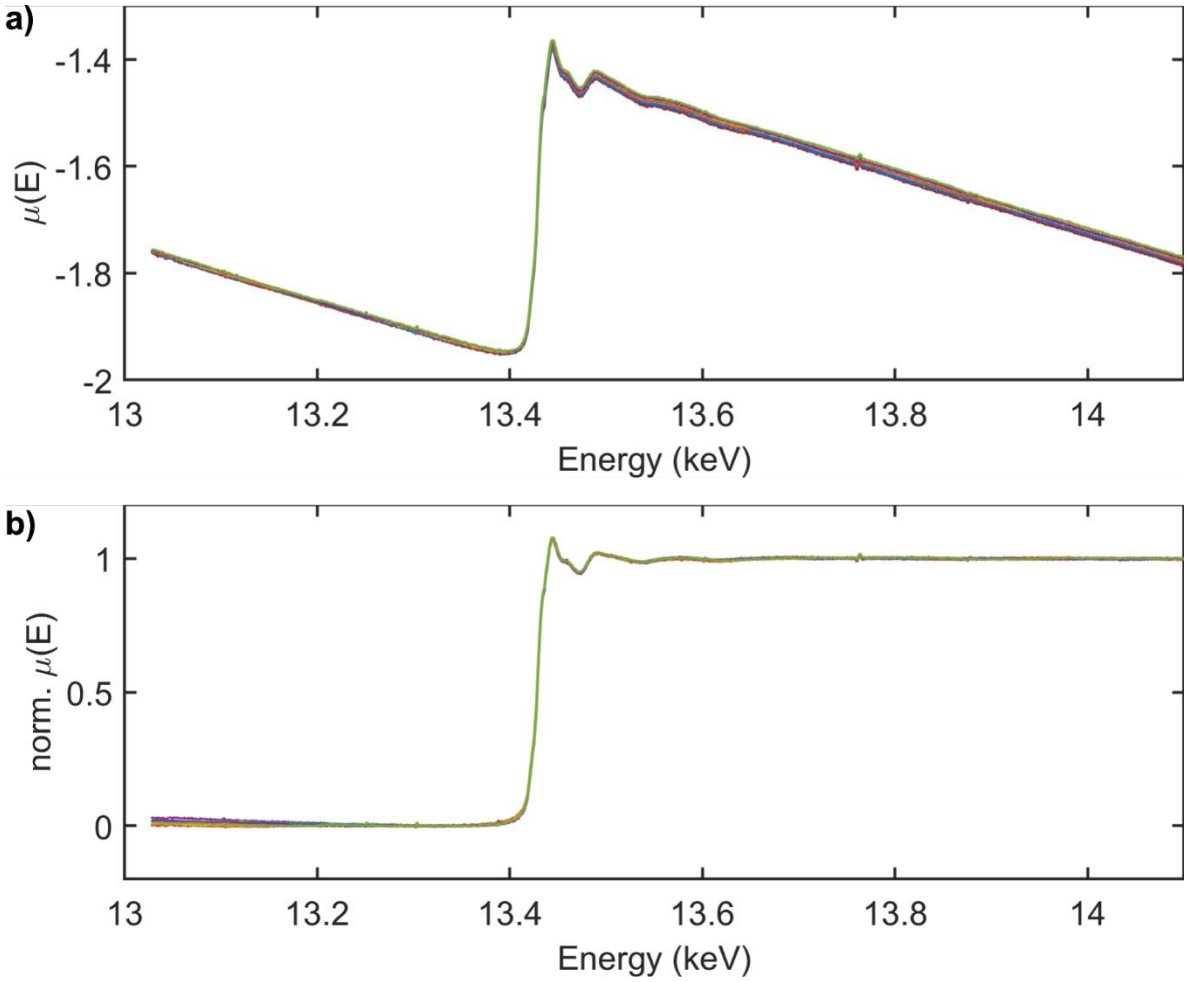

Fig. S6. XAFS data acquired in the LRC. a) 12 Absorption spectra of $Bi_{24}O_{31}Cl_{10}$ plotted on top of each other to show the consistency between different spectra. b) Energy calibrated and normalized absorption spectra of $Bi_{24}O_{31}Cl_{10}$ from a). These data form basis of the data plots in Fig. S5.

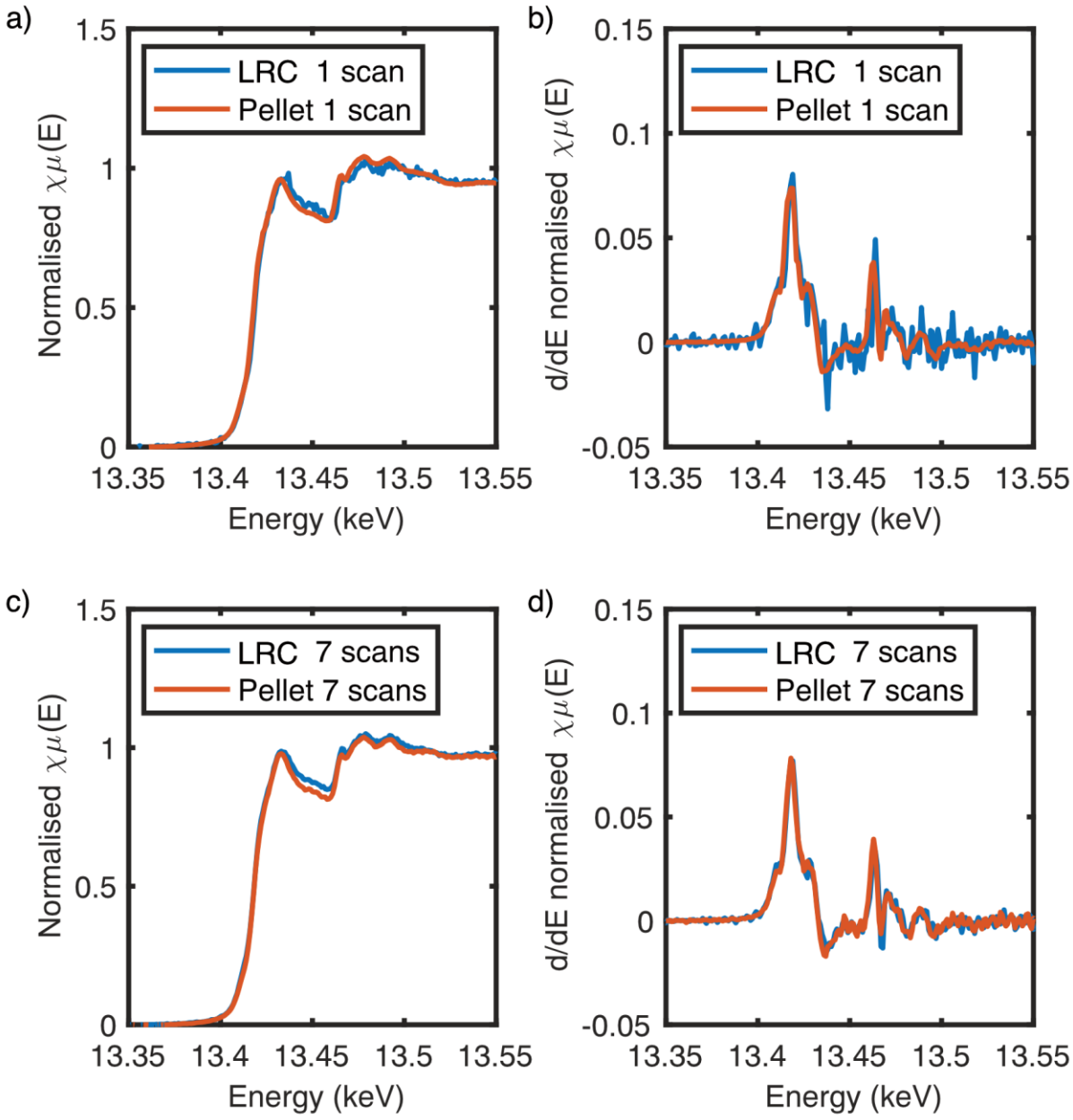

Fig. S7. Smoothened XANES spectra collected at the Bi L^{III} edge on $Bi_{24}O_{31}Br_{10}$ in the LRC (blue) compared to a pellet (red). In a) single XANES scans are compared, and the first derivative of these spectra are shown in b). The noise level is high for the LRC data in comparison with the pellet. c) The average of seven XANES spectra, and d) the first derivative of the spectra in c). The noise is reduced considerably by averaging over seven spectra.

5. Light-driven reaction

On Balder at the MAX IV Laboratory, the LiquidReactionCell was tested for its potential to follow a light-driven process. Prior to data collection, a suspension of $Bi_{24}O_{31}Br_{10}$ in isopropanol was bubbled with argon to remove all air. After bubbling, the suspension was irradiated with a Thorlab 455 nm LED at a light intensity of 1 sun for approx. 1.5 hours, while XAS data were collected. In agreement with previous findings under inert conditions[2,3], the yellow material turned black as a result of hydrogenation of the catalyst surface (Fig. S8). Unfortunately, the reaction did not result in changes in the spectra. We suggest this is due to the majority of the particle volume remaining unchanged in this process, or the bismuth coordination to be largely unaffected by the reduction.

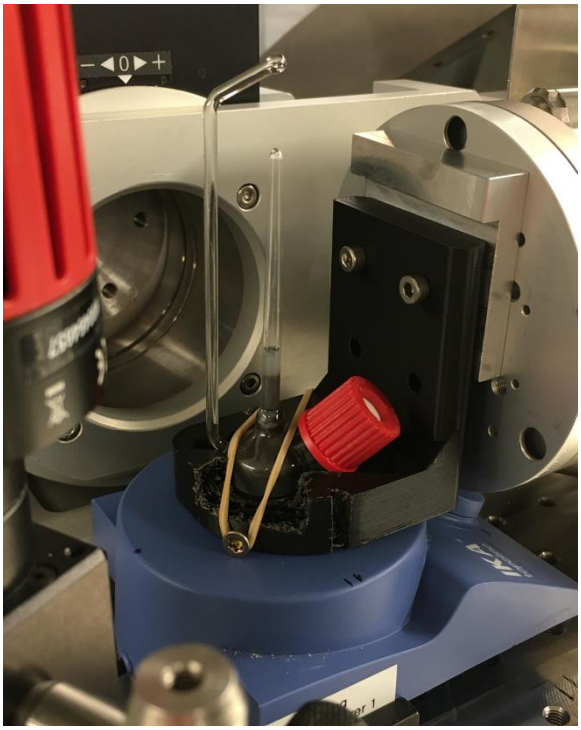

Fig. S8. Hydrogenated $Bi_{24}O_{31}Br_{10}$ in isopropanol suspension in the LRC in argon atmosphere after illumination on Balder at the MAX IV Laboratory. The sample prior to irradiation is shown in Fig. 2d in the manuscript.

6. Total scattering and Pair Distribution Function

6.1 Total scattering patterns of suspension in the LRC

In Fig. S9, the collected intensities (blue), background intensities (black) and background corrected pattern (red) is shown. The patterns used in the waterfall plots shown in Fig. S10 are all background corrected similarly to the red pattern here.

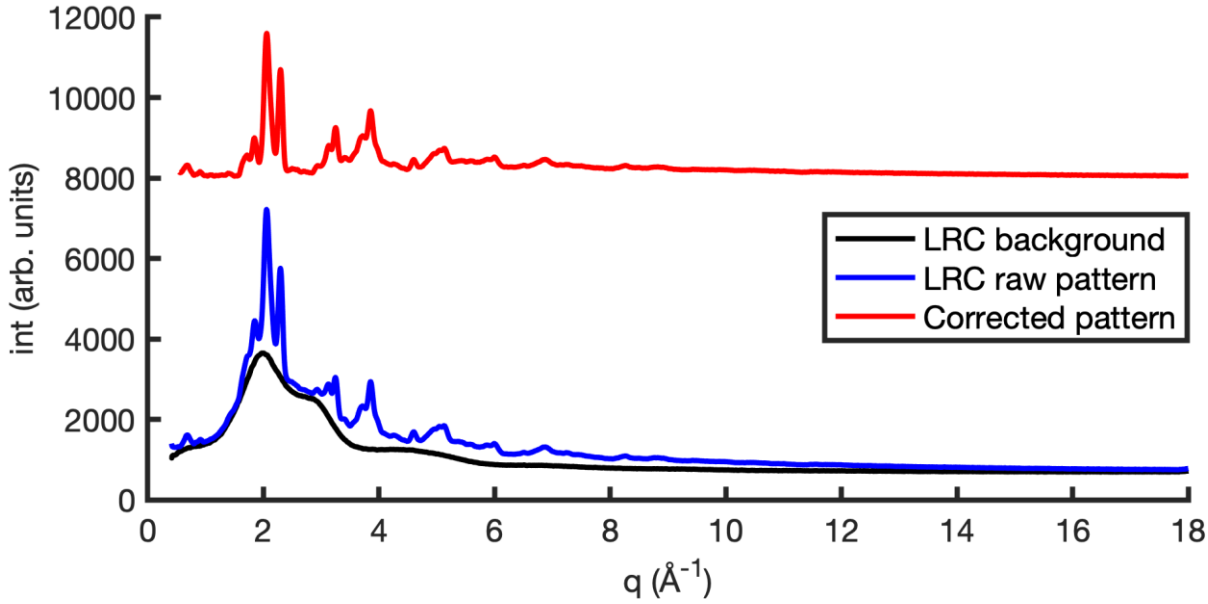

Fig. S9. Integrated total scattering data collected on a suspension of $Bi_{24}O_{31}Cl_{10}$ in the LRC. The scattering intensities of water and the LRC is shown in black, the data of $Bi_{24}O_{31}Cl_{10}$ in water suspension in the cell is shown in blue. The background corrected pattern is shown in red.

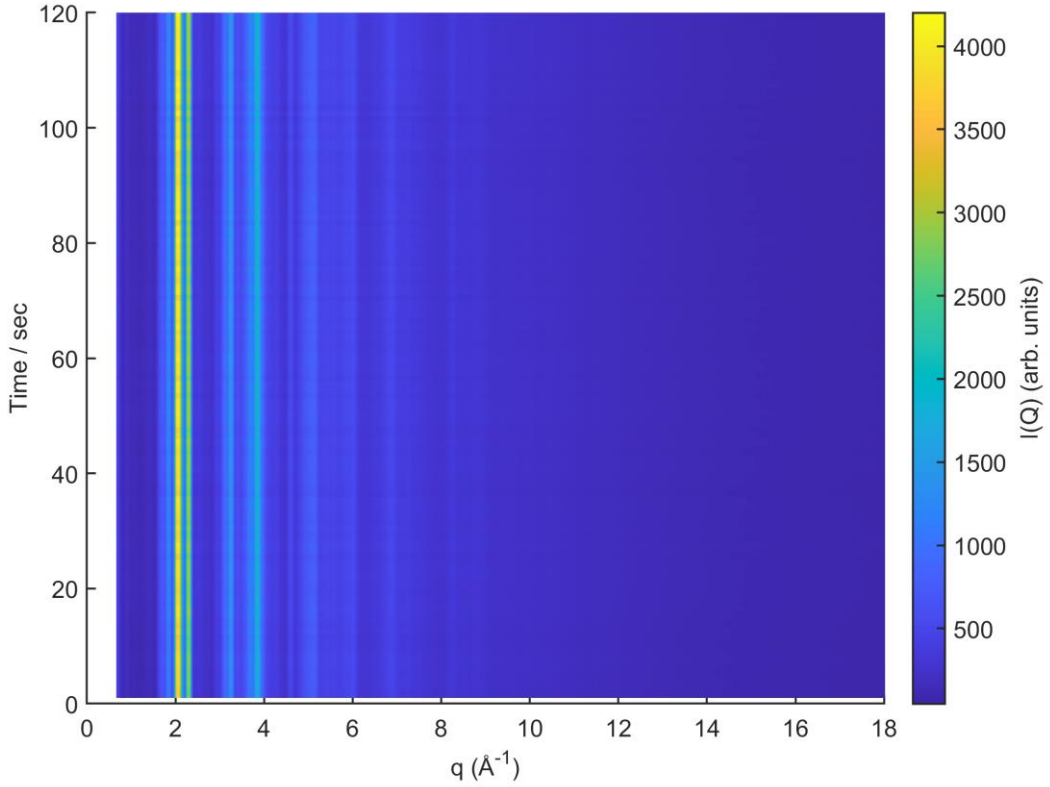

Fig. S10. Top view of the waterfall plot of the background corrected intensities collected on $Bi_{24}O_{31}Cl_{10}$ in suspension (1 s exposures).

Fig. S11 shows an enlarged waterfall plots of the PDFs seen in the manuscript Fig. 5b.

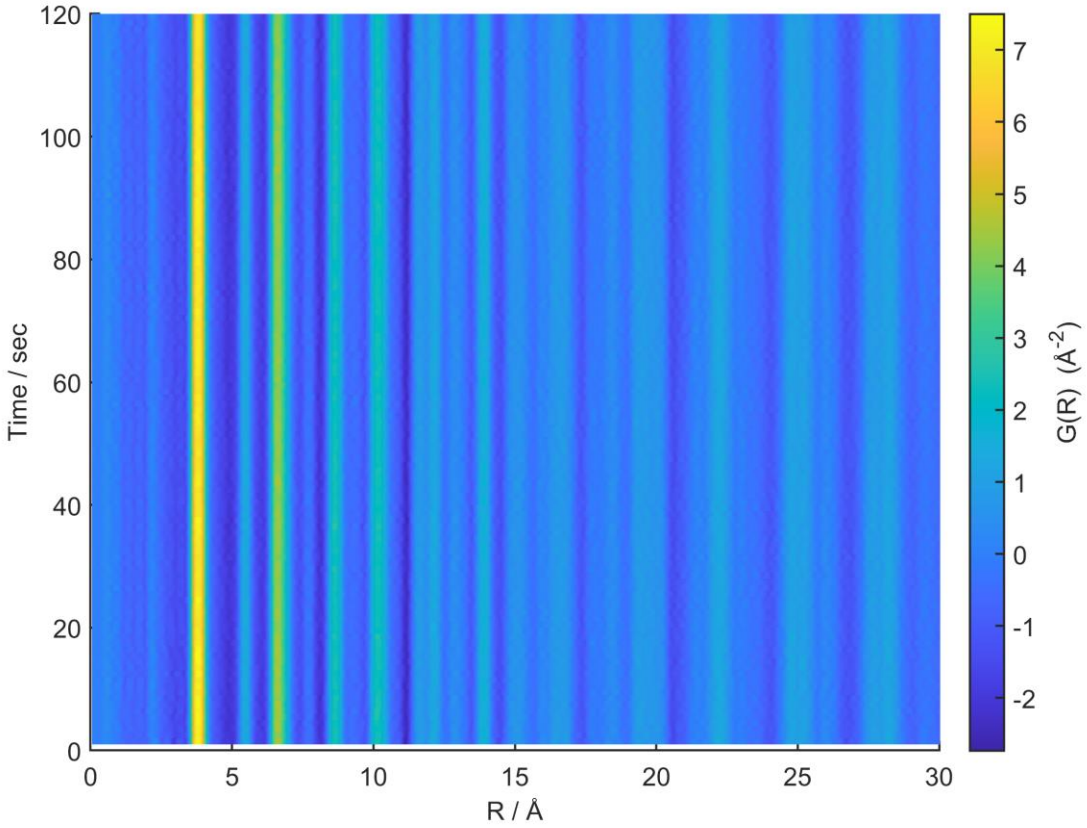

Fig. S11. Waterfall plot of $G(r)$ over 120 s with 1 s exposures, revealing the overall uniformity of the suspension in LRC over time.

6.2 Real space Rietveld refinement of $Bi_{24}O_{31}Cl_{10}$ PDF

Rietveld refinements were performed in PDFgui. The parameters Q_{damp} (0.02912 $Å^{-1}$) and Q_{broad} (0.002654 $Å^{-1}$) were determined from data collected on LaB_6 in a capillary, and these values were fixed during the refinement of LRC data.

In the refinements of $Bi_{24}O_{31}Cl_{10}$, the scale factor, unit cell axes length, β-angle, and SPdiameter were refined. The thermal parameters were described isotopically ($U_{11}=U_{22}=U_{33}$), and $U_{Bi}=U_O$ were refined independently from U_{Cl} to accommodate the difference in their chemical environment (see structural drawing in the manuscript Fig. 1; Bi and O comprises bismuth oxide layers while the Cl ions are located in-between). Finally, all delta2 values were not refined and fixed to a value of 2

The resulting fits are shown in Fig. S12, and the refined parameters are shown in Table S2.

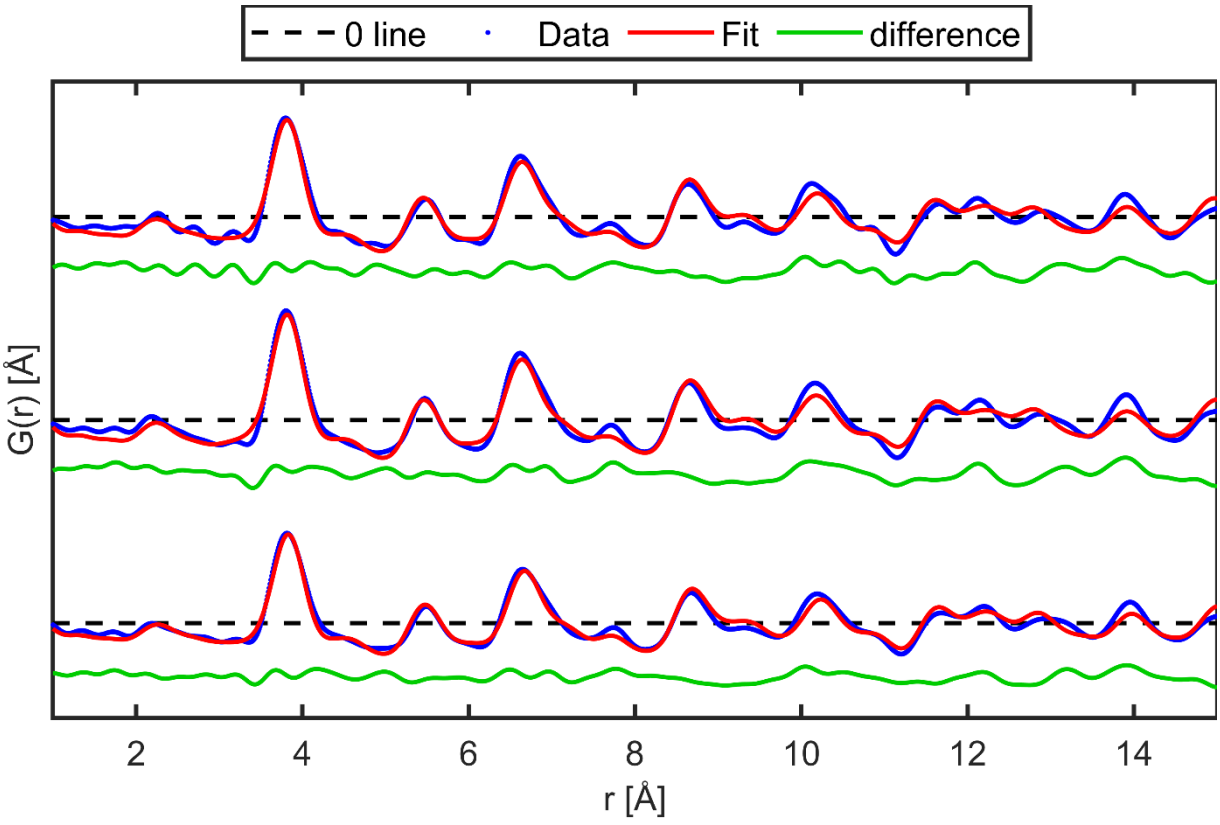

Fig. S12: PDF fits of $Bi_{24}O_{31}Cl_{10}$ from measurements in the LRC at 1 s exposure (top), LRC at 60 s exposure (middle), and in a capillary at 60 s exposure (bottom). The individual plots are stacked and each plot have a zero-line added in dashes as a guide for the eye.

Table S2: Refined parameters from refinements in PDFGui. Please note the errors are not physical errors, but mathematical errors as the former are not yet possible to obtain.

	Capillary 60 s		**LRC 60 s**		**LRC 1 s**	
	value	**error**	**value**	**error**	**value**	**error**
Scale	1.062	0.039	1.34	0.04	1.214	0.038
a (Å)	29.58	0.12	29.647	0.074	29.49	0.09
b (Å)	3.874	0.019	3.83	0.01	3.844	0.013
c (Å)	10.253	0.031	10.267	0.029	10.247	0.031
β (degrees)	88.0	0.4	88.58	0.29	88.57	0.34
SPdiameter (Å)	38.6	3.9	34.2	2.5	35.4	2.7
$U_{\mathrm{Bi/O}}$ (Å^2)	0.01532	0.0009	0.0078	0.00085	0.0160	0.0009
U_{Cl} (Å^2)	0.234	0.083	0.245	0.027	0.194	0.064
Reduced χ^2	0.120		0.236		0.189	
R_{w}	0.227		0.258		0.254	

6.3 *In situ* formation of copper hydroxide at P21.1, PETRA III

A test of the potential to follow a chemical reaction *in situ* in the LRC was performed at P21.1 at PETRA III, by collection of total scattering data. The formation of copper hydroxide nanoparticles was followed by the addition of $NaOH_{(aq)}$ to a copper sulphate solution.

The LRC was set up in a similar way to the experiments at P02.1, PETRA III (see Section 1.2). A Perkin Elmer XRD1621 detector was used in full ring configuration with a wavelength of 0.1222 Å (101.5 keV) and a sample-to-detector distance of 353 mm. All data was saved in 1 s frames integrated and later merged into 5 s patterns before they were transformed to $G(r)$ using a Q_{max} of 18 $Å^{-1}$ and rpoly of 1.4.

To accommodate the addition of $NaOH_{(aq)}$, two needles were inserted through the injection tube: one for inlet flow of the base and one outlet needle to keep the volume constant within the LRC. Additionally, an Ocean QE PRO XR UV/VIS spectrometer was placed externally at the top of the suspension in the X-ray Illuminated Zone as shown in Fig S13a making sure the fibre optic probes were levelled with the X-ray beam path. All regular light sources were turned off during the measurement, such no stray light would be picked up by the UV/VIS.

The LRC was filled with 0.5 M $CuSO_4 \cdot 5H_2O_{(aq)}$ and sealed. Using a New Era syringe pump (NE-1000), 2 mL NaOH solution (10 M) was injected to the LRC at 0.5 mL/min slowly forming a light blue suspension. The injection was started at 110 s.

As seen in Fig S13b, the UV/VIS clearly shows an initial absorption spectrum representative of the blue $CuSO_4$ solution, which disappears around t=240 s as the suspension starts forming. However, $G(r)$ in Fig. S13c reveals that no new correlations are forming until t=280 s, where longer range correlations start forming indicative of nanoparticle formation. Interestingly, the time between the loss of absorption to the formation of copper hydroxide nanoparticles indicate an intermediate phase, which does not alter the local structure of the precursor. However, a deeper discussion of the chemistry is out of the scope of this paper.

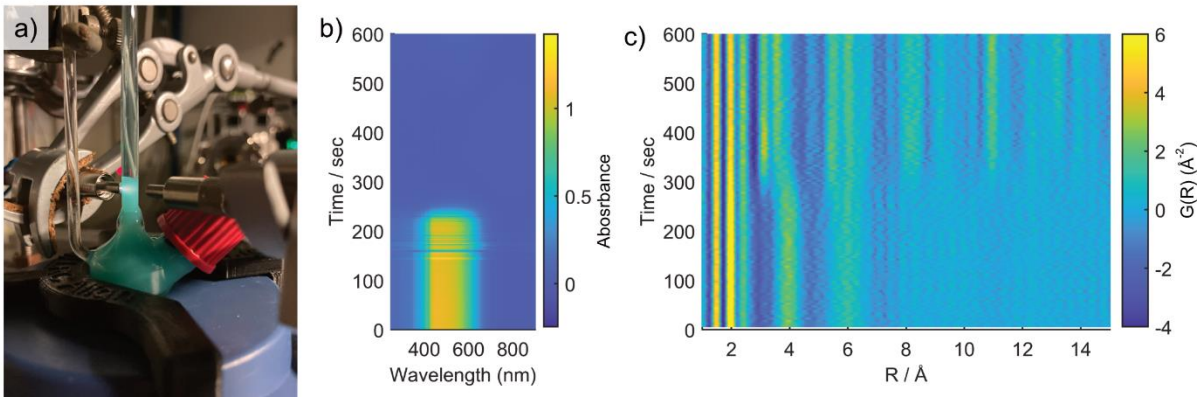

Fig. S13: a) LRC placed at P21.1, PETRA III with UV/VIS probes on either side of the X-ray Illuminated Zone. b) UV/VIS absorption spectra displayed in 1 s frames. c) $G(r)$ of the copper hydroxide formation displayed in 5 s frames.

7. References

1 M. J. Berger, J. H. Hubbell, S. M. Seltzer, J. Chang, J. S. Coursey, R. Sukumar, D. S. Zucker and K. Olsen, XCOM: Photon Cross Sections Database (version 1.5).

2 Y. Dai, C. Li, Y. Shen, S. Zhu, M. S. Hvid, L. C. Wu, J. Skibsted, Y. Li, J. W. H. Niemantsverdriet, F. Besenbacher, N. Lock and R. Su, *J. Am. Chem. Soc.*, 2018, **140**, 16711–16719.

3 Y. Dai, P. Ren, Y. Li, D. Lv, Y. Shen, Y. Li, H. Niemantsverdriet, F. Besenbacher, H. Xiang, W. Hao, N. Lock, X. Wen, J. P. Lewis and R. Su, *Angew. Chem. Int. Ed.*, 2019, **58**, 6265–6270.